Progress in PHOTOVOLTAICS

PROGRESS IN PHOTOVOLTAICS: RESEARCH AND APPLICATIONS
Prog. Photovolt: Res. Appl. 2014; **22**:277–282
Published online 13 January 2014 in Wiley Online Library (wileyonlinelibrary.com). DOI: 10.1002/pip.2475

ACCELERATED PUBLICATION

Wafer bonded four-junction GaInP/GaAs//GaInAsP/GaInAs concentrator solar cells with 44.7% efficiency

Frank Dimroth[1]*, Matthias Grave[1], Paul Beutel[1], Ulrich Fiedeler[1], Christian Karcher[1], Thomas N. D. Tibbits[1], Eduard Oliva[1], Gerald Siefer[1], Michael Schachtner[1], Alexander Wekkeli[1], Andreas W. Bett[1], Rainer Krause[2], Matteo Piccin[2], Nicolas Blanc[2], Charlotte Drazek[2], Eric Guiot[2], Bruno Ghyselen[2], Thierry Salvetat[3], Aurélie Tauzin[3], Thomas Signamarcheix[3], Anja Dobrich[4], Thomas Hannappel[4†] and Klaus Schwarzburg[4]

[1] Fraunhofer Institute for Solar Energy Systems ISE, Heidenhofstr. 2, 79110 Freiburg, Germany
[2] SOITEC S.A., Parc Technologique des Fontaines, 38190 Bernin, France
[3] CEA LETI MINATEC campus, 17 rue des Martyrs, 38054 Grenoble, France
[4] Helmholtz-Zentrum Berlin HZB, Hahn-Meitner-Platz 1, 14109 Berlin, Germany

ABSTRACT

Triple-junction solar cells from III–V compound semiconductors have thus far delivered the highest solar-electric conversion efficiencies. Increasing the number of junctions generally offers the potential to reach even higher efficiencies, but material quality and the choice of bandgap energies turn out to be even more importance than the number of junctions. Several four-junction solar cell architectures with optimum bandgap combination are found for lattice-mismatched III–V semiconductors as high bandgap materials predominantly possess smaller lattice constant than low bandgap materials. Direct wafer bonding offers a new opportunity to combine such mismatched materials through a permanent, electrically conductive and optically transparent interface. In this work, a GaAs-based top tandem solar cell structure was bonded to an InP-based bottom tandem cell with a difference in lattice constant of 3.7%. The result is a GaInP/GaAs//GaInAsP/GaInAs four-junction solar cell with a new record efficiency of 44.7% at 297-times concentration of the AM1.5d (ASTM G173-03) spectrum. This work demonstrates a successful pathway for reaching highest conversion efficiencies with III–V multi-junction solar cells having four and in the future even more junctions. Copyright © 2014 John Wiley & Sons, Ltd.

KEYWORDS
concentrator cells; multi-junction solar cells; wafer bonding; III–V semiconductors

***Correspondence**
Frank Dimroth, Fraunhofer Institute for Solar Energy Systems, Heidenhofstr. 2, 79110 Freiburg, Germany.
E-mail: frank.dimroth@ise.fraunhofer.de
[†]Present address: TU Ilmenau, Ehrenbergstraße 29, 98693 Ilmenau, Germany

Received 25 October 2013; Revised 10 December 2013; Accepted 18 December 2013

1. INTRODUCTION

Today's industry standard solar cell for concentrator applications is a triple-junction cell made of $Ga_{1-x}In_xP$ (1.8–1.9 eV), $Ga_{1-y}In_yAs$ (1.3–1.4 eV), and Ge (0.7 eV). This type of solar cell has reached record efficiencies up to 41.6% under concentrated sunlight illumination and is produced by several companies [1–3]. In the case of the lattice matched $Ga_{0.49}In_{0.51}P/Ga_{0.99}In_{0.01}As/Ge$ material combination, the Ge bottom junction is known to generate a large excess current, which limits the device performance. Furthermore, the Ge cell suffers of a comparably low current and voltage performance. More advanced triple-junction solar cells have therefore used III–V compounds with bandgaps of around 1.0 eV instead of Ge. Examples are dilute nitride semiconductors like GaInNAs [4] or inverted metamorphic GaInAs [5]. These solar cells reach efficiencies up to 44.4 % at 302 sun concentration [6,7]. The performance can be further improved by adding additional junctions. The theoretical optimum for a four-junction solar cell under AM1.5d spectral conditions is reached for a set of declining bandgap energies with 1.9, 1.4, 1.0, and 0.5 eV. In 2011, a combination close to this theoretical optimum was realized with a GaInP/GaAs/GaInNAs/Ge four-junction cell, [8] but the performance of this device was not satisfactory due to insufficient quality of the dilute

nitride material grown by metal-organic-vapor-phase-epitaxy. More promising results were reported for inverted metamorphic devices [9] reaching AM0 (space solar spectrum) one-sun efficiencies up to 33.6%. In this configuration, two lattice-mismatched $Ga_{1-x}In_xAs$ bottom junctions are combined with a $Ga_{0.5}In_{0.5}P$/GaAs top tandem by using buffer layers to relax the crystal lattice. Dislocations cannot be completely avoided in this configuration, and this leads to constraints in device performance. Wafer bonding is another technology to combine lattice-mismatched materials without creating dislocations. Two crystal structures are brought closely together forming atomic bonds at the interface [10,11]. This technology requires two epitaxial structures with low surface roughness and a specific surface preparation of the materials but offers the advantage of combining the best defect-free semiconductors in a multi-junction solar cell device. Wafer bonding has been used by several authors in the past [12–15], but the present work, for the first time, presents results of a four-junction device, which is at the level of the best triple-junction solar cells. This is achieved by a $Ga_{0.51}In_{0.49}P$/GaAs top tandem bonded to a $(Ga_{0.16}In_{0.84})(As_{0.31}P_{0.69})$/$Ga_{0.47}In_{0.53}As$ bottom tandem solar cell (Figure 1). This combination is close to the ideal bandgap combination for a four-junction device and allows one to reach excellent material quality for all junctions.

2. EXPERIMENTAL

The epitaxial growth of the III–V compound semiconductor layer structure was performed by metal-organic vapor phase epitaxy in an Aixtron 2800-G4 TM reactor with an 8 × 4-inch configuration at Fraunhofer ISE. Two separate growth runs led to an inverted $Ga_{0.51}In_{0.49}P$/GaAs top tandem cell on GaAs and an upright $(Ga_{0.16}In_{0.84})(As_{0.31}P_{0.69})$/$Ga_{0.47}In_{0.53}As$ bottom tandem cell structure on InP. The diameter of the substrates was 100 mm in both cases. The overall layer structure for the four-junction solar cell contains the four pn-junctions, and an additional number of barrier and tunnel diode layers between the subcells. All junctions were grown lattice matched to the underlying substrate, which avoids formation of dislocations and ensures outstanding material quality. Highly doped n-type layers of GaAs and InP with $N_D > 10^{18}\,cm^{-3}$ were used at the bond interface. The high doping level is beneficial for a low resistance of the bond interface. This is especially important for the application of solar cells under concentrated sunlight illumination where typically current densities of 5–10 A/cm^2 are flowing through this device.

The top and bottom tandem solar cells were polished to obtain a root mean square surface roughness below 0.3 nm, which was confirmed by atomic force microscopy measurements on a typical area of $5 \times 5\,\mu m^2$. The two wafers were then cleaned and brought into close contact, and the wafer bond was initiated. After post-bond annealing, stable bonds are formed between the atoms on both sides of the interface. All process steps for the bonding were prepared by the Soitec and CEA-LETI team in a class 100 cleanroom facility using proprietary SmartCut technology experience.

It is important to avoid contamination of the wafers before the bonding as particles may cause large bonding defects. Figure 2 shows a scanning acoustic microscope image of the bonded solar cell wafer pair. Two circles with a clear white contrast in the microscope image are likely due to particles formed during epitaxy or handling of the

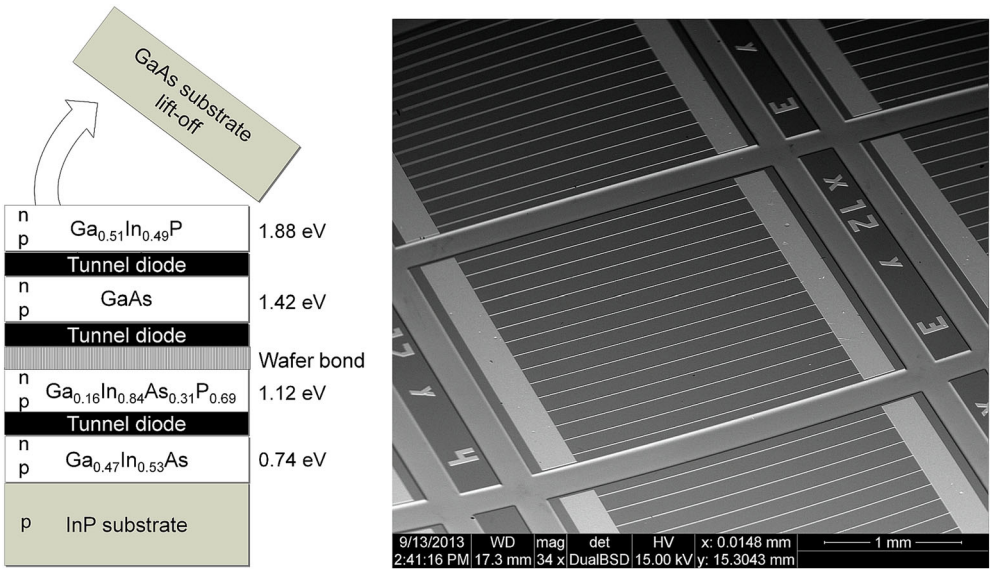

Figure 1. Schematic layer structure of the four-junction wafer bonded solar cell (left) indicating the composition of the subcell materials with bandgap energies, the location of tunnel diodes and the wafer bond. Scanning electron microscopy image of the concentrator cell design with a designated area of 5.2 mm^2 (right). The bonded solar cell had two terminals with parallel grid fingers and two rectangular shaped busbars forming the front contact.

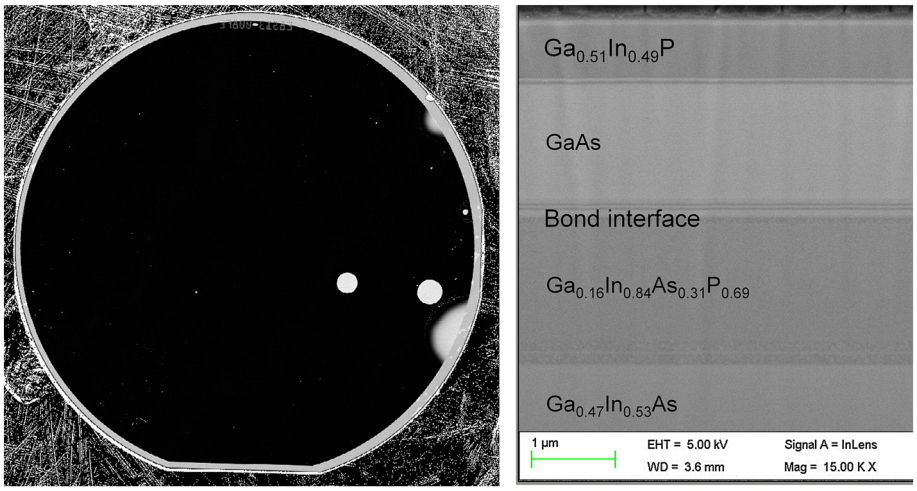

Figure 2. Scanning acoustic microscope image of the two bonded wafer pairs forming the GaInP/GaAs//GaInAsP/GaInAs structure (left). The bond location, indicated by a double slash //, is formed between the GaAs and GaInAsP subcells. The GaAs and InP substrates have not yet been removed before the measurement. Non-bonded areas at the interface are detected as white contrast. Cross-section scanning electron microscopy images of the bonded four-junction solar cell structure (right) give no indication of crystal defects at the bond interface.

wafers. Most of the wafer surface was successfully bonded, and scanning electron microscopy images of a solar cell cross-section reveal no indication of defects at the interface (Figure 2 (right)). The conductivity of the bond has been analyzed and a low resistance of $<10\,\mathrm{mOhm\,cm^2}$ was confirmed, suitable for the operation of the solar cell under high concentration.

After the wafer bonding, the GaAs substrate was removed by wet chemical etching, and ohmic front and back side contacts were applied at Fraunhofer ISE. The front metal contacts had a finger width of 5 µm, resulting in low shadowing losses. A MgF_2/TaO_x two layer anti-reflection coating was evaporated onto a 25 nm thick AlInP window layer forming the front-side passivation of the $Ga_{0.51}In_{0.49}P$ top cell. All solar cells were finally separated by a wet chemical mesa etch. Several hundred solar cell devices were processed on a full 100 mm wafer. The area of the cells was varying between $5.2\,\mathrm{mm^2}$ and $4\,\mathrm{cm^2}$.

Quantum efficiencies [16] and IV characteristics were measured in the Fraunhofer ISE CalLab using a spectrally adjustable solar simulator to measure the IV characteristics under one-sun AM1.5d ($1000\,\mathrm{W/m^2}$, 25 °C) standard test conditions. The setup of the solar simulator and the test procedure are described in more detail in reference [17]. The performance of the devices under concentration was determined by the use of a Xe-flash simulator with adjustable distance between the flash bulb and the measurement plane. Because of the small area of the concentrator solar cells, the efficiency depends significantly on the correct measurement of the mesa area. This was done with high precision using a LEXT laser confocal microscope.

Finally, the electroluminescence (EL) emission spectrum of the four solar cell junctions at 298 K was measured with four individual mini spectrometers which are coupled to the solar cell via optical fibers. The EL signal of the two high bandgap junctions was investigated with Si detector arrays. Two additional GaInAs detector arrays were used for the measurement of the low bandgap subcells. The procedure of determining the individual subcell voltages from the EL spectrum at different current densities follows the references [18,19].

3. RESULTS AND DISCUSSION

Solar cell structures for the InP-based and GaAs-based tandem devices were grown separately and investigated before joining them together as a four-junction cell. Epitaxy process parameters were optimized to achieve high quantum efficiencies in all subcells and to ensure high peak tunnel current densities $>20\,\mathrm{A/cm^2}$ for the tunnel diodes. Figure 3 shows the absolute external quantum efficiency (EQE) of the best wafer bonded GaInP/GaAs//GaInAsP/GaInAs four-junction solar cell device. The current under the AM1.5d ASTM G173-03 spectrum is limited by the GaInP top subcell with a calibrated photocurrent density of $12.42\,\mathrm{mA/cm^2}$ (see IV curve in Figure 4). The other subcell currents are calculated from the EQE to be $12.60\,\mathrm{mA/cm^2}$ for GaAs, $12.54\,\mathrm{mA/cm^2}$ for GaInAsP, and $13.69\,\mathrm{mA/cm^2}$ for the GaInAs bottom cell. This leads to an excess current density of 10% for the bottom GaInAs cell. The junction thicknesses and bandgap energies may be controlled more precisely in the future to adjust for this remaining current mismatch, which leads to losses due to the series-connection of the subcells. Furthermore, the EQE of the GaAs second subcell can be increased if the tunnel diode layers above the cell are exchanged from the current p-$Al_{0.3}Ga_{0.7}As$ and n-GaAs to a more transparent set of semiconductors.

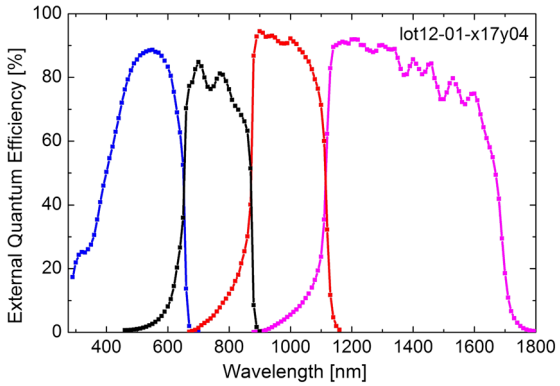

Figure 3. Absolute external quantum efficiency of the best four-junction GaInP/GaAs//GaInAsP/GaInAs solar cell (sample name Lot12-01-x17y04). The measurement was performed on the 5.2 mm^2 concentrator solar cell device.

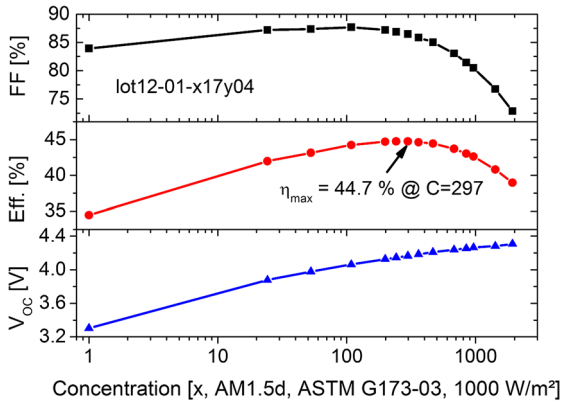

Figure 5. Summary of IV characteristics under concentration for the best four-junction GaInP/GaAs//GaInAsP/GaInAs solar cell (sample name Lot12-01-x17y04) with an area of 5.2 mm^2. The efficiency maximum of 44.7% is reached at 297 suns. All measurements were performed by the Fraunhofer ISE CalLab at T = 25 °C.

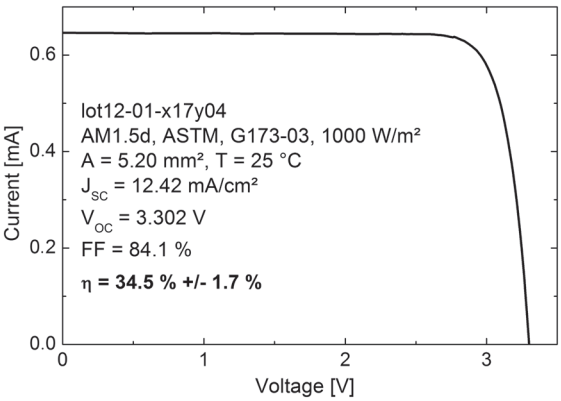

Figure 4. IV curve for the best four-junction GaInP/GaAs//GaInAsP/GaInAs solar cell (sample name Lot12-01-x17y04) at one-sun AM1.5d, ASTM, G173-03, 25 °C. The measurement was performed by the Fraunhofer ISE CalLab using a spectrally matched solar simulator.

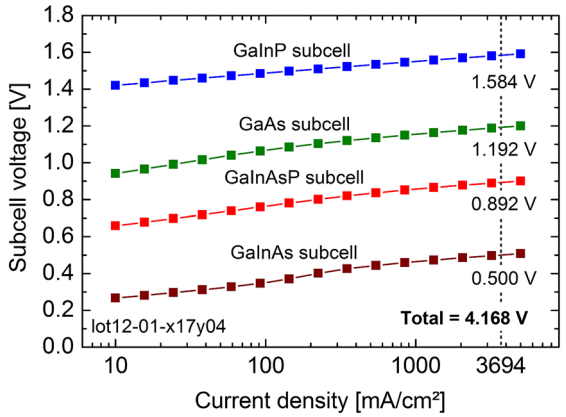

Figure 6. Subcell voltages derived from the electroluminescence measurement of a four-junction GaInP/GaAs//GaInAsP/GaInAs solar cell as a function of the applied current density.

The EQE of the GaInAsP junction shows a significant overlap with the GaAs subcell in the wavelength range between 700 and 900 nm. This confirms the high transparency of the bond interface, an important advantage of direct wafer bonding, which does not require additional materials for the bonding and therefore leads to zero absorption and low interface reflection due to the smooth transition between GaAs and InP with similar refractive indices. Also, the high EQE of the GaInAsP cell indicates excellent crystal quality, which is not degraded by the bonding.

The IV characteristics of the best GaInP/GaAs//GaInAsP/GaInAs concentrator solar cell have been determined as a function of concentration. Figure 4 shows the calibrated IV curve at one-sun AM1.5d ASTM G173-3 together with values for the short-circuit current density J_{sc}, the open-circuit voltage V_{oc}, fill factor FF, and efficiency η. The fill factor increases under concentration (Figure 5) and peaks at 100 suns before series-resistance losses start to dominate at high current densities. The highest conversion efficiency is reached at 297 suns concentration with a value of 44.7 ± 3.1%. The efficiency remains high in a broad concentration range from 100 to 1000 suns with a measured value of 42.6 ± 3.0% at 962 suns. No indication of a breakdown of the tunnel diodes is observed at high concentration levels.

The voltages of the four subcells have been analyzed by EL spectroscopy. Figure 6 shows the calculated open-circuit voltages as a function of the current densities. The maximum efficiency is reached at a concentration of 297 suns, which is equivalent to a current density of 3694 mA/cm^2. Under these conditions, the subcell voltages are determined to be 1.584 V (GaInP), 1.192 V (GaAs), 0.892 V (GaInAsP), and 0.500 V (GaInAs). The difference E_g-qV_{oc} between the bandgap energy of the semiconductor and the product of elementary charge q times the open-circuit voltage of the device is a

good indicator for material quality and the ideality of the diodes. The GaInP top cell shows the largest offset in voltage of 296 mV, followed by the GaInAs bottom cell with 240 mV and the two GaAs and GaInAsP middle cells with 228 mV. There is still potential to improve the quality of these top and bottom junctions in the future.

4. CONCLUSIONS

This paper presents results of a wafer bonded four-junction solar cells with a peak efficiency of 44.7% at 297 suns concentration. Wafer bonding allows the defect-free combination of two GaAs-based and InP-based tandem solar cell structures with a lattice mismatch of 3.7 %. More than 90% of the substrate area with a diameter of 100 mm was bonded successfully and showed no indication of interface defects such as voids. The peak external quantum efficiency was above 80% for all subcells. Notably, the high voltage and current of the GaInAsP junction directly below the bond interface confirms the excellent transparency of the bond and the achievement of low bulk defect densities. The solar cells can be operated up to high concentration levels of several thousand suns without any indication of tunnel diode breakdown, and the high performance of 42.6% efficiency at 962 suns is further indication for the low resistance of the bond interface. The solar cell structure still offers significant potential for improvements as some of the largest losses are due to an absorbing AlGaAs/GaAs tunnel diode between the GaInP and GaAs subcell, a current mismatch of 10% and a low voltage of the GaInP top cell.

ACKNOWLEDGEMENTS

The authors like to acknowledge device processing and characterization by M. Scheer, K. Wagner, A. Panamatschuk, E. Fehrenbacher, T. Gandy, K. Mayer, I. Semke, and E. Schäffer. We also like to thank Emmanuelle Lagoutte (CEA-LETI), Jocelyne Wasselin (Soitec), Chantal Arena (Soitec), and Fred Newman (Soitec) for very valuable discussions. Soitec and CEA-LETI would like to acknowledge support from the French Environment and Energy Management Agency (ADEME) through the "Investissement d'Avenir" program GUEPARD.

REFERENCES

1. Guter W, Kern R, Köstler W, Kubera T, Löckenhoff R, Meusel M, Shirnow M, Strobl G. III-V multijunction solar cells - new lattice-matched products and development of upright metamorphic 3 j cells. in *7th International Conference on Concentrating Photovoltaic Systems*. 2011. Las Vegas, Nevada, USA: AIP Conference Proceedings. p. 5–8.
2. Ermer JH, Jones RK, Hebert P, Pien P, King RR, Bhusari D, Brandt R, Al-Taher O, Fetzer C, Kinsey GS, Karam N. Status of C3MJ + and C4MJ production concentrator solar cells at Spectrolab. *IEEE Journal of Photovoltaics* 2012; **2**(2): 209–213.
3. King RR, Bhusari D, Larrabee D, Liu XQ, Rehder E, Edmondson K, Cotal H, Jones RK, Ermer JH, Fetzer CM, Law DC, Karam NH. Solar cell generations over 40% efficiency. *Progress in Photovoltaics: Research and Applications* 2012; **20**: 801–815.
4. Sabnis V, Yuen H, Wiemer M. High-efficiency multijunction solar cells employing dilute nitrides. in *8th International Conference on Concentrating Photovoltaic Systems*. 2012. Toledo, Spain: AIP Conference Proceedings. p. 14–19.
5. Geisz JF, Friedman DJ, Ward JS, Duda A, Olavarria WJ, Moriarty TE, Kiehl JT, Romero MJ, Norman AG, Jones KM. 40.8% efficient inverted triple-junction solar cell with two independently metamorphic junctions. *Applied Physics Letters* 2008; **93**(12): 123501–123505.
6. Sasaki K, Agui T, Nakaido K, Takahashi N, Onitsuka R, Takamoto T. Development of InGaP/GaAs/InGaAs inverted triple junction concentrator solar cells. in *9th International Conference on Concentrator Photovoltaic Systems*. 2013. Miyazaki, Japan: AIP Conference Proceedings. p. 22–25.
7. Green MA, Emery K, Hishikawa Y, Warta W, Dunlop ED. Solar cell efficiency tables (version 42). *Progress in Photovoltaics: Research and Applications* 2013; **21**: 827–837.
8. Essig S, Stämmler E, Rönsch S, Oliva E, Schachtner M, Siefer G, Bett AW, Dimroth F. Dilute nitrides for 4- and 6- junction space solar cells. in *Proceedings of the 9th European Space Power Conference*. 2011. Saint-Raphael, France.
9. Stan M, Aikena D, Choa B, Cornfelda A, Leya V, Patela P, Sharpsa P, Varghese T. High-efficiency quadruple junction solar cells using OMVPE with inverted metamorphic device structures. *Journal of Crystal Growth* 2010; **312**(8): 1370–1374.
10. Goesele U, Alexe M, Kopperschmidt P, Tong Q-Y. Semiconductor wafer bonding. *Annual Review of Materials Science* 1998; **28**: 215–241.
11. Moriceau H, Rieutord F, Fournel F, Le Tiec Y, Di Cioccio L, Morales C, Charvet AM, Deguet C. Overview of recent direct wafer bonding advances and applications. *Advances in Natural Sciences: Nanoscience and Nanotechnology* 2010; **1**: 043004.
12. Tanabe K, Aiken DJ, Wanlass MW, Fontcuberta i Morral A, Atwater HA. Lattice-mismatched monolithic GAAS/INGAAS two-junction solar cells by direct wafer bonding. in *Proceedings of the 4th World Conference on Photovoltaic Energy Conversion*. 2006. Waikoloa, Hawaii, USA. p. 768–771.

13. Law DC, King RR, Yoon H, Archer MJ, Boca A, Fetzer CM, Mesropian S, Isshiki T, Haddad M, Edmondson KM, Bhusari D, Yen J, Sherif RA, Atwater HA, Karam NH. Future technology pathways of terrestrial III-V multijunction solar cells for concentrator photovoltaic systems. *Solar Energy Materials and Solar Cells* 2008; **94**: 1314–1318.
14. Bhusari D, Law D, Woo R, Boisvert J, Mesropian S, Larrabee D, Hong HF, Karam NH. Direct semiconductor bonding technology (SBT) for high efficiency III-V multi-junction solar cells. in *Proceedings of the 37th IEEE Photovoltaic Specialists Conference*. 2011. Seattle, Washington, USA. p. 1–4.
15. Derendorf K, Essig S, Oliva E, Klinger V, Roesener T, Philipps SP, Benick J, Hermle M, Schachtner M, Siefer G, Jäger W, Dimroth F. Fabrication of GaInP/GaAs//Si solar cells by surface activated direct wafer bonding. *IEEE Journal of Photovoltaics* 2013; **3**(4): 1423–1428.
16. Meusel M, Baur C, Létay G, Bett AW, Warta W, Fernandez E. Spectral response measurements of monolithic GaInP/Ga(In)As/Ge triple-junction solar cells: measurement artifacts and their explanation. *Progress in Photovoltaics: Research and Applications* 2003; **11**(8): 499–414.
17. Meusel M, Adelhelm R, Dimroth F, Bett AW, Warta W. Spectral mismatch correction and spectrometric characterization of monolithic III-V multi-junction solar cells. *Progress in Photovoltaics: Research and Applications* 2002; **10**(4): 243–255.
18. Rau U. Reciprocity relation between photovoltaic quantum efficiency and electroluminescent emission of solar cells. *Physical Review B* 2007; **76**: 085301–085303.
19. Rönsch S, Hoheisel R, Dimroth F, Bett AW. Subcell I-V characteristic analysis of GaInP/GaInAs/Ge solar cells using electroluminescence measurements. *Applied Physics Letters* 2011; **98**(25): 251113.